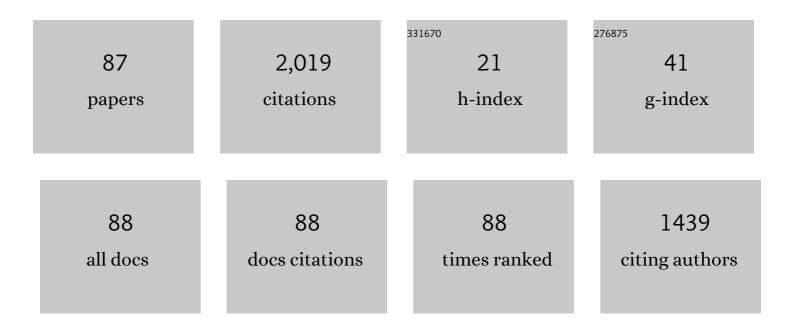
List of Publications by Year in descending order

Source: https://exaly.com/author-pdf/3517635/publications.pdf Version: 2024-02-01



#	Article	IF	CITATIONS
1	Fuel design and management for the control of advanced compression-ignition combustion modes. Progress in Energy and Combustion Science, 2011, 37, 741-783.	31.2	462
2	Premixed low-temperature combustion of blends of diesel and gasoline in a high speed compression ignition engine. Proceedings of the Combustion Institute, 2011, 33, 3039-3046.	3.9	142
3	Attainment and Load Extension of High-Efficiency Premixed Low-Temperature Combustion with Dieseline in a Compression Ignition Engine. Energy & Fuels, 2010, 24, 3517-3525.	5.1	95
4	Structural and Biochemical Characterization Reveals LysCH15 as an Unprecedented "EF-Hand-Like― Calcium-Binding Phage Lysin. PLoS Pathogens, 2014, 10, e1004109.	4.7	85
5	Experimental study on compound HCCI (homogenous charge compression ignition) combustion fueled with gasoline and diesel blends. Energy, 2014, 64, 707-718.	8.8	78
6	A new methodology for diesel surrogate fuel formulation: Bridging fuel fundamental properties and real engine combustion characteristics. Energy, 2018, 148, 424-447.	8.8	76
7	An experimental study of injection and spray characteristics of diesel and gasoline blends on a common rail injection system. Energy, 2014, 75, 513-519.	8.8	41
8	Chemical Mechanism of Exhaust Gas Recirculation on Polycyclic Aromatic Hydrocarbons Formation Based on Laser-Induced Fluorescence Measurement. Energy & Fuels, 2018, 32, 7112-7124.	5.1	39
9	Combustion and emissions of isomeric butanol/gasoline surrogates blends on an optical GDI engine. Fuel, 2020, 272, 117690.	6.4	39
10	Experimental study on injection characteristics of fatty acid esters on a diesel engine common rail system. Fuel, 2014, 123, 19-25.	6.4	38
11	Long-term system load forecasting based on data-driven linear clustering method. Journal of Modern Power Systems and Clean Energy, 2018, 6, 306-316.	5.4	36
12	Octane rating effects of direct injection fuels on dual fuel HCCI-DI stratified combustion mode with port injection of n-heptane. Energy, 2016, 111, 1003-1016.	8.8	33
13	Macroscopic and microscopic spray characteristics of fatty acid esters on a common rail injection system. Fuel, 2017, 203, 370-379.	6.4	32
14	Numerical study on fuel physical effects on the split injection processes on a common rail injection system. Energy Conversion and Management, 2017, 134, 47-58.	9.2	31
15	Experimental and modeling validation of a large diesel surrogate: Autoignition in heated rapid compression machine and oxidation in flow reactor. Combustion and Flame, 2019, 202, 195-207.	5.2	29
16	Autoignition of <i>n</i> -Hexane, Cyclohexane, and Methylcyclohexane in a Constant Volume Combustion Chamber. Energy & Fuels, 2019, 33, 3576-3583.	5.1	27
17	Influences of isomeric butanol addition on anti-knock tendency of primary reference fuel and toluene primary reference fuel gasoline surrogates. International Journal of Engine Research, 2021, 22, 39-49.	2.3	27
18	Experimental study of the two-stage injection process of fatty acid esters on a common rail injection system. Fuel, 2016, 163, 214-222.	6.4	25

#	Article	IF	CITATIONS
19	Laminar flame propagation and nonpremixed stagnation ignition of toluene and xylenes. Proceedings of the Combustion Institute, 2017, 36, 479-489.	3.9	24
20	Exergy losses in auto-ignition processes of DME and alcohol blends. Fuel, 2018, 229, 116-125.	6.4	24
21	Hydrolyzed polyacrylamide biotransformation in an up-flow anaerobic sludge blanket reactor system: key enzymes, functional microorganisms, and biodegradation mechanisms. Bioprocess and Biosystems Engineering, 2019, 42, 941-951.	3.4	24
22	Impact of Short-Range Clustering on the Multistage Work-Hardening Behavior in Cu–Ni Alloys. Metals, 2019, 9, 151.	2.3	22
23	Second-law thermodynamic analysis for premixed hydrogen flames with diluents of argon/nitrogen/carbon dioxide. International Journal of Hydrogen Energy, 2019, 44, 5020-5029.	7.1	21
24	Size evolution of soot particles from gasoline and n-heptane/toluene blend in a burner stabilized stagnation flame. Fuel, 2017, 203, 135-144.	6.4	20
25	Effect of mixing methane, ethane, propane and ethylene on the soot particle size distribution in a premixed propene flame. Combustion and Flame, 2018, 193, 54-60.	5.2	20
26	Autoignition of n-heptane and butanol isomers blends in a constant volume combustion chamber. Fuel, 2019, 254, 115638.	6.4	20
27	Experimental study on dual-fuel compound homogeneous charge compression ignition combustion. International Journal of Engine Research, 2013, 14, 23-33.	2.3	19
28	Experimental study on the two stage injection of diesel and gasoline blends on a common rail injection system. Fuel, 2015, 159, 470-475.	6.4	18
29	Nozzle effects on the injection characteristics of diesel and gasoline blends on a common rail system. Energy, 2018, 153, 223-230.	8.8	18
30	Analysis of exergy losses in laminar premixed flames of methane/hydrogen blends. International Journal of Hydrogen Energy, 2019, 44, 24043-24053.	7.1	18
31	Cetane number prediction for hydrocarbons from molecular structural descriptors based on active subspace methodology. Fuel, 2019, 249, 1-7.	6.4	18
32	Dilution, Thermal, and Chemical Effects of Carbon Dioxide on the Exergy Destruction in n-Heptane and Iso-octane Autoignition Processes: A Numerical Study. Energy & Fuels, 2018, 32, 5559-5570.	5.1	17
33	Second-Law Thermodynamic Analysis in Premixed Flames of Ammonia and Hydrogen Binary Fuels. Journal of Engineering for Gas Turbines and Power, 2019, 141, .	1.1	17
34	A comparative study on soot particle size distributions in premixed flames of RP-3 jet fuel and its surrogates. Fuel, 2020, 259, 116222.	6.4	17
35	Rural-Spatial Restructuring Promoted by Land-Use Transitions: A Case Study of Zhulin Town in Central China. Land, 2021, 10, 234.	2.9	17
36	Numerical study on explosion limits of ammonia/hydrogen/oxygen mixtures: Sensitivity and eigenvalue analysis. Fuel, 2021, 300, 120964.	6.4	17

#	Article	IF	CITATIONS
37	A six-component surrogate of diesel from direct coal liquefaction for spray analysis. Fuel, 2018, 234, 1259-1268.	6.4	16
38	Exergy loss characteristics of DME/air and ethanol/air mixtures with temperature and concentration fluctuations under HCCI/SCCI conditions: A DNS study. Combustion and Flame, 2021, 226, 334-346.	5.2	15
39	Autoignition Comparison of <i>n</i> -Dodecane/Benzene and <i>n</i> -Dodecane/Toluene Blends in a Constant Volume Combustion Chamber. Energy & Fuels, 2019, 33, 5647-5654.	5.1	13
40	Effects of butanol blending on spray auto-ignition of gasoline surrogate fuels. Fuel, 2020, 260, 116368.	6.4	13
41	Evaluating the impact of smart grid technologies on generation expansion planning under uncertainties. International Transactions on Electrical Energy Systems, 2016, 26, 934-951.	1.9	11
42	Hydraulic dynamics in split fuel injection on a common rail system and their artificial neural network prediction. Fuel, 2019, 255, 115792.	6.4	11
43	Numerical study on exergy losses of iso-octane constant-volume combustion with water addition. Fuel, 2019, 248, 127-135.	6.4	11
44	The synthesis and characterization of glutathione-modified superparamagnetic iron oxide nanoparticles and their distribution in rat brains after injection in substantia nigra. Journal of Materials Science: Materials in Medicine, 2019, 30, 5.	3.6	11
45	MicroRNA-23a suppresses the apoptosis of inflammatory macrophages and foam cells in atherogenesis by targeting HSP90. Gene, 2020, 729, 144319.	2.2	11
46	Prediction of Standard Enthalpies of Formation Based on Hydrocarbon Molecular Descriptors and Active Subspace Methodology. Industrial & Engineering Chemistry Research, 2020, 59, 4785-4791.	3.7	11
47	Influence of Fuel Supply Timing and Mixture Preparation on the Characteristics of Stratified Charge Compression Ignition Combustion with N-Heptane Fuel. Combustion Science and Technology, 2009, 181, 1327-1344.	2.3	10
48	Applicability of high dimensional model representation correlations for ignition delay times of n-heptane/air mixtures. Frontiers in Energy, 2019, 13, 367-376.	2.3	10
49	An experimental study on spray auto-ignition of RP-3 jet fuel and its surrogates. Frontiers in Energy, 2021, 15, 396-404.	2.3	10
50	Combustion and emissions of RP-3 jet fuel and diesel fuel in a single-cylinder diesel engine. Frontiers in Energy, 2023, 17, 664-677.	2.3	10
51	Dilution, Thermal and Chemical Effects of Carbon Dioxide on n-heptane Two-Stage Auto-Ignition Process. , 0, , .		9
52	Active fuel design—A way to manage the right fuel for HCCI engines. Frontiers in Energy, 2016, 10, 14-28.	2.3	9
53	An experimental and modeling study on the low-temperature oxidation of methylcyclopentane in a jet-stirred reactor. Fuel, 2021, 293, 120374.	6.4	9
54	Synthesis and properties of fluorinated <scp>benzotriazoleâ€based donorâ€acceptorâ€type</scp> conjugated polymers via <scp>Pdâ€catalyzed</scp> direct <scp>Cï£;H</scp> / <scp>Cï£;H</scp> coupling polymerization. Journal of Polymer Science, 2021, 59, 240-250.	3.8	9

#	Article	IF	CITATIONS
55	Effects of Exhaust Gas Recirculation Constituents on Methyl Decanoate Auto-Ignition: A Kinetic Study. Journal of Engineering for Gas Turbines and Power, 2018, 140, .	1.1	8
56	Effects of mechanism reduction on the exergy losses analysis in n-heptane autoignition processes. International Journal of Engine Research, 2020, 21, 1764-1777.	2.3	8
57	Effects of fuel combination and IVO timing on combustion and emissions of a dual-fuel HCCI combustion engine. Frontiers in Energy, 2020, 14, 778-789.	2.3	8
58	Gasoline octane number prediction from near-infrared spectroscopy with an ANN-based model. Fuel, 2022, 318, 123543.	6.4	8
59	Second-law thermodynamic analysis on non-premixed counterflow methane flames with hydrogen addition. Journal of Thermal Analysis and Calorimetry, 2020, 139, 2577-2583.	3.6	7
60	Size Distribution of Soot Particles in Premixed <i>n</i> -Heptane and Methylcyclohexane Flames. Energy & Fuels, 2018, 32, 3883-3890.	5.1	6
61	Exergy losses in premixed flames of dimethyl ether and hydrogen blends. Frontiers in Energy, 2019, 13, 658-666.	2.3	6
62	Size Distribution of Nascent Soot in Premixed <i>n</i> -Hexane, Cyclohexane, and Methylcyclohexane Flames. Energy & Fuels, 2019, 33, 5740-5748.	5.1	6
63	A strategy for iron oxide nanoparticles to adhere to the neuronal membrane in the substantia nigra of mice. Journal of Materials Chemistry B, 2020, 8, 758-766.	5.8	6
64	Spray Auto-ignition Behaviors of Diesel and Jet Fuel at Reduced Oxygen Environments. Combustion Science and Technology, 2020, , 1-15.	2.3	6
65	Soot particle size distributions in premixed flames of RP-3 jet fuel and its distillates. Fuel, 2020, 267, 117244.	6.4	6
66	Influences of C5 esters addition on anti-knock and auto-ignition tendency of a gasoline surrogate fuel. International Journal of Engine Research, 2022, 23, 1782-1791.	2.3	6
67	Effects of branch structure of alkylbenzenes on spray auto-ignition of <i>n</i> -decane and alkylbenzenes blends. International Journal of Engine Research, 2021, 22, 1636-1651.	2.3	5
68	Fuel octane number prediction based on topological indices and active subspace method. Fuel, 2021, 293, 120494.	6.4	4
69	Numerical study on the physical and chemical processes in n-decane spray ignition. Chemical Engineering Science, 2021, 241, 116716.	3.8	4
70	An experimental and modeling study on polyoxymethylene dimethyl ether 3 (PODE3) oxidation in a jet stirred reactor. Fundamental Research, 2022, 2, 738-747.	3.3	4
71	Attachment of streptavidin-modified superparamagnetic iron oxide nanoparticles to the PC-12 cell membrane. Biomedical Materials (Bristol), 2020, 15, 045014.	3.3	4
72	The influence of spatial interfaces on rural economic restructuring in rapidly industrializing areas: A case study of Gongyi city in central China. Growth and Change, 0, , .	2.6	4

#	Article	IF	CITATIONS
73	1,2-Dimyristoyl- <i>sn-glycero</i> -3-phosphocholine promotes the adhesion of nanoparticles to bio-membranes and transport in rat brain. RSC Advances, 2021, 11, 35455-35462.	3.6	4
74	Comparative Study on Spray Auto-Ignition of Di-n-Butyl Ether and Diesel Blends at Engine-Like Conditions. Journal of Energy Resources Technology, Transactions of the ASME, 2021, 143, .	2.3	4
75	Soot size distribution in lightly sooting premixed flames of benzene and toluene. Frontiers in Energy, 2020, 14, 18-26.	2.3	3
76	A robust optimization approach to evaluate the impact of smart grid technologies on generation plans. , 2014, , .		2
77	Recent progress and challenges in process optimization: Review of recent work at ECUST. Canadian Journal of Chemical Engineering, 2018, 96, 2115-2123.	1.7	2
78	Application of Active Subspace Method in Gas Exchange Strategy Calibration on a Variable Valve Timing Gasoline Engine. Journal of Engineering for Gas Turbines and Power, 2020, 142, .	1.1	2
79	Development and Production of High Rate MRPC for CBM TOF. , 2019, , .		2
80	Theoretical study on isomerization, decomposition and ring-closure reaction kinetics of methyl pentanoate radicals. Combustion and Flame, 2022, 237, 111848.	5.2	2
81	Elesesterpenes A–K: Lupane-type Triterpenoids From the Leaves of Eleutherococcus sessiliflorus. Frontiers in Chemistry, 2021, 9, 813764.	3.6	2
82	Effects of equivalence ratio and carbon dioxide concentration on premixed charge compression ignition of gasoline and diesel-like fuel blends. Journal of Mechanical Science and Technology, 2013, 27, 2507-2512.	1.5	1
83	Risk assessment model for wind power integrated power systems using conditional value-at-risk. , 2014, , .		1
84	Pressure-Based Approach to Estimating the Injection Start and End in Single and Split Common Rail Injection Processes. Journal of Shanghai Jiaotong University (Science), 2018, 23, 28-33.	0.9	1
85	Second-law thermodynamic analysis on premixed syngas flames. International Journal of Exergy, 2020, 32, 174.	0.4	1
86	Spatiotemporal Evolution of Specialized Villages in the Yellow River Basin and Its Influencing Factors. Papers in Applied Geography, 0, , 1-18.	1.4	1
87	An analytical method for quantitative reconstruction of X-ray fluorescence computed tomography with attenuation correction. , 2015, , .		0